Impact of Load Frequency Dependence on the NDZ and Performance of the SFS Islanding Detection Method

H. H. Zeineldin, *Member, IEEE*, and M. M. A. Salama, *Fellow, IEEE*

***Abstract*—Sandia frequency shift (SFS) falls under the active islanding detection methods that rely on frequency drift to detect an islanding condition for inverter-based distributed generation. Active islanding detection methods are commonly tested on constant RLC loads where the load's active power is directly proportional to the square of voltage and is independent on the system frequency. Since the SFS method relies primarily on frequency to detect islanding, the load's active power frequency dependence could have an impact on its performance and the nondetection zone (NDZ). In this paper, the impact of the load's active power frequency dependence on the performance of the SFS method, during an islanding condition, is analyzed. A NDZ model that takes into account the load's frequency dependence parameter is derived mathematically and validated through digital simulation. The results show that the load's frequency dependence has a significant impact on the NDZ of the SFS method and thus is an important factor to consider when designing and testing this method.**

***Index Terms*—Distributed generation (DG), inverter, islanding detection, Sandia frequency shift (SFS).**

I. Introduction

ANTIISLANDING protection is an essential component to consider when integrating distributed generation (DG) to distribution systems. The main role of an islanding detection method is to detect accurately the moment of islanding and then isolate the DG in a timely manner. Islanding detection methods could be classified into three main groups which include passive, active and communication based [1]–[3]. Passive methods rely on setting an upper and lower threshold on a certain measured parameter, for example, frequency or voltage, to detect an islanding condition [1]–[4]. In active methods, the interface control design is modeled such that a certain system parameter is forced to drift once an islanding condition occurs and thus facilitating islanding detection [5], [6]. Recently, new active methods, relying on injecting disturbances, were proposed to detect an islanding condition [6], [7]. In [6], the proposed method relies on injecting a negative sequence current and measuring the corresponding negative sequence voltage variation to detect islanding. In [7], the current angle signal is distorted by injecting a low amplitude sinusoidal waveform and measuring the corresponding voltage deviation. Communication-based methods rely on sending and receiving signals between different protective devices to detect islanding. Active methods are considered the most attractive option since active methods are less expensive than communication based and have smaller nondetection zone (NDZ) than passive methods. NDZ could be defined as the loading conditions for which an islanding detection method would fail to detect islanding in a timely manner [8]. Recently, hybrid passive-active islanding detection methods combining advantages of both approaches were proposed in [9]–[11].

Sandia frequency shift (SFS) falls under the frequency drift active methods which also includes active frequency drift (AFD) [12], automatic phase shift, and slip mode frequency shift (SMS) [13]. The NDZ of active methods, relying on frequency drift, was analyzed in [14] and [15]. The SFS method was proven to be one of the most effective methods with a small NDZ. Islanding detection methods, and their NDZ, were developed and tested on constant RLC loads [1]–[9], [11]–[18]. In [19], the effect of the load's frequency dependence on the operation of one of the passive methods, over/under voltage protection and over/under frequency protection, was analyzed, and it was concluded that the load's frequency dependence has an impact of the NDZ and islanding detection capability of this method [19].

Commonly in power system transient analysis, the load frequency dependence is taken into account and has a major effect on the frequency deviation [20]–[23]. This has not been taken into consideration in the design of active methods such as the SFS method. The SFS method was tested on constant RLC loads which were assumed to be the hardest loading condition to detect [15]. Loads, on a distribution system, vary in characteristic depending on the type (residential, commercial or industrial) as well as season and weather [21]. In [21], typical load frequency dependence parameters were given for various types of loads. The majority of the loads operate close to unity power factor with the active power frequency dependence parameter varying from 0 to 3 [20].

In this paper, the performance of the SFS method is tested taking into account the load's frequency dependence. The NDZ for the SFS method is derived mathematically to demonstrate

Manuscript received May 24, 2009; revised July 31, 2009; accepted September 15, 2009. Date of publication October 6, 2009; date of current version December 10, 2010.

H. H. Zeineldin is with the Masdar Institute of Science and Technology, Abu Dhabi, United Arab Emirates (e-mail: hzainaldin@masdar.ac.ae).

M. M. A. Salama is with the Electrical and Computer Engineering Department, University of Waterloo, Waterloo, ON N2L 3G1, Canada, and also with King Saud University, Riyadh 11451, Saudi Arabia (e-mail:msalama@hivolt.uwaterloo.ca).

Color versions of one or more of the figures in this paper are available online at http://ieeexplore.ieee.org.

Digital Object Identifier 10.1109/TIE.2009.2033482

TABLE I
TYPICAL LOAD FREQUENCY DEPENDENCE PARAMETER

Load Type	k_{pf}
3–phase Air condition	0.98
Water Heater	0
Clothes Washer	3
Fluorescent lights	1
Fan motors	2.9
Agricultural pump	5

the effect of load frequency dependence parameter on islanding detection. The inverter-based DG as well as the islanding detection method is modeled on PSCAD/EMTDC and simulation results are presented to verify the mathematical analysis. This paper is organized as follows: Section II derives the mathematical expression used to model the NDZ. Section III analyzes the effect of load frequency dependence on the performance of the SFS method. Section IV provides simulation results to verify the mathematical analysis. Lastly, conclusions are drawn in Section V.

II. NDZ WITH FREQUENCY DEPENDENT LOADS

The NDZ of an islanding detection method could be represented in the $\Delta P-\Delta Q$ (active power mismatch–reactive power mismatch), $L-C_{\rm norm}$ (load inductance–load normalized capacitance), or Q_f-f_r (load quality factor–load resonance frequency) plane [8], [14], [15]. In this paper, the $\Delta P-\Delta Q$ is implemented and new equations are derived, for modeling the NDZ that take into account the active power frequency dependence. The load is represented by a parallel inductance (L), capacitance (C), and a resistance (R) that is frequency dependent to model active power frequency dependence. The load characteristic can depend on the season, class (residential, commercial, or industrial) and composition of the load (air conditions, lighting, electric heating, and motor loads). For example, the typical active power load frequency dependence parameter for a residential electrical heating load during the summer and winter are 0.7 and 1, respectively [21]. Typical load frequency parameters could be found in [21].

Generally, in order to determine the load parameters, measurement, and data acquisition devices are installed at the load terminal. These devices measure voltage and frequency deviations during a disturbance event. The corresponding variation in load active and reactive power is measured, and the load model is estimated by fitting the data to the assumed model. Table I presents the active power load frequency dependence values for various types of loads [20].

In general, the load's active and reactive power can be modeled in terms of R, L, and C as follows:

$$P=(P_o+\Delta P)\left(\frac{V}{V_o}\right)^{NP}(1+k_{\rm pf}(f-f_o))=\frac{3V^2}{R} \quad (1)$$

$$Q_L=(Q_o+\Delta Q)=\frac{3V_o^2}{\omega_o L} \quad (2)$$

$$Q_C=Q_o=3V_o^2\omega_o C \quad (3)$$

where P, Q_L, and Q_C represent the load's active, inductive reactive, and capacitive reactive three phase power, respectively, and ΔP and ΔQ represent the active and reactive power mismatch, respectively. The term NP represents the load's voltage dependence parameter which will be set equal to two while $k_{\rm pf}$ represents the load's frequency dependence parameter. The parameters V, V_o, and ω_o represent the system operating voltage, system nominal voltage, and system nominal frequency in radians per second, respectively. The parameters f and f_o represent the system frequency and nominal frequency, respectively. To represent the NDZ in terms of ΔP, the load and DG power are equated as follows:

$$P_{\rm DG}=P_{\rm Load}. \quad (4)$$

The DG is designed to operate as a constant current-controlled source. For the SFS method, the DG phase angle is expressed as follows:

$$\phi_{\rm DG}=-\frac{\pi}{2}\left(cf+k(f-f_o)\right) \quad (5)$$

where cf and k represent the parameters of the SFS islanding detection method. The SFS method relies on injecting a slightly distorted current waveform in order to drift the frequency beyond the frequency relay threshold values presented in the IEEE standards [17], [24], [25]. This is accomplished by chopping the current waveform, through the parameter cf, and introducing zero periods which will in turn affect the DG phase angle. In addition to cf, the DG phase angle is designed to be dependent on the system frequency by introducing another factor "k" [14], [15]. By referring to (4), the active power balance equation could be expressed as follows:

$$3VI_{\rm rated}\cos\phi_{\rm DG}=(P_o+\Delta P)\left(\frac{V}{V_o}\right)^{NP}(1+k_{\rm pf}(f-f_o)) \quad (6)$$

where $I_{\rm rated}$ is the DG rated output current. Equation (6) can be further simplified as shown in

$$\frac{P_o}{\cos\phi_{\rm DG|rated}}V\cos\phi_{\rm DG}$$

$$=(P_o+\Delta P)\left(\frac{V}{V_o}\right)^{NP}(1+k_{\rm pf}(f-f_o))\,V_o \quad (7)$$

$$\frac{\Delta P}{P_o}$$

$$=\frac{\cos\phi_{\rm DG}}{\left(\frac{V}{V_o}\right)^{NP-1}(1+k_{\rm pf}(f-f_o))\cos[\phi_{\rm DG|rated}]}-1. \quad (8)$$

Equation (8) represents the main equation for determining the active power mismatch term for modeling the NDZ. It can be seen that the NDZ will be dependent on $k_{\rm pf}$. The reactive power mismatch can be found by equating the DG and load reactive power as follows:

$$3VI_{\rm rated}\sin\phi_{\rm DG}=Q_L-Q_C=\frac{3V^2}{\omega L}-3V^2\omega C. \quad (9)$$

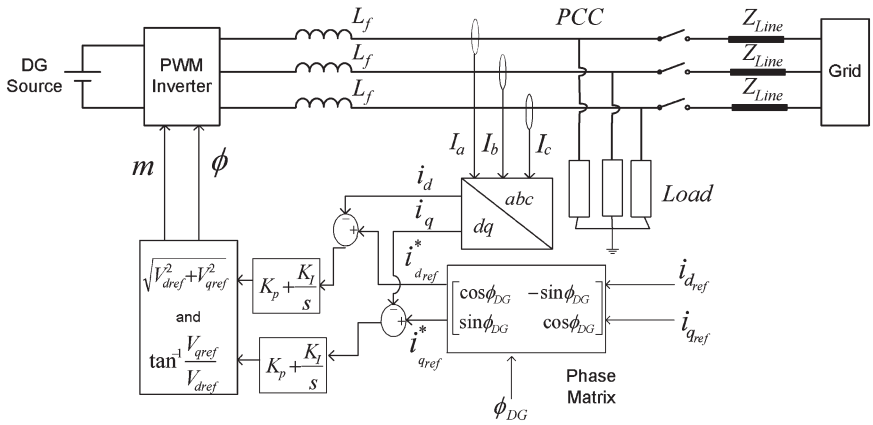

Fig. 1. System under study.

By substituting for the values of C and L from (2) and (3) and after a sequence of simplifications, (9) can be rewritten as follows:

$$\frac{\omega}{\omega_o}\frac{\Delta P}{P_o}\left(1+k_{\rm pf}(f-f_o)\right)\tan\phi_{\rm DG}-\frac{\Delta Q}{P_o} = \frac{Q_0}{P_o}\left(1-\frac{\omega^2}{\omega_o^2}\right)-\frac{\omega}{\omega_o}\left(1+k_{\rm pf}(f-f_o)\right)\tan\phi_{\rm DG}. \quad (10)$$

Equation (10) represents the main equation for determining the NDZ in terms of reactive power mismatch. Equations (8) and (10) will be used in this paper to construct the NDZ of the SFS islanding detection method in the $\Delta P-\Delta Q$ *space*.

III. Effect of Load Frequency Dependence on the NDZ of the SFS Islanding Detection Method

The system under study is shown in Fig. 1 which consists of a distribution system represented by a source behind an impedance, a 100-kW inverter-based DG and a load. The load resistance is modeled as in (1) to simulate a frequency dependent load. Islanding studies are commonly performed on DG equipped with inverters that are designed to provide no voltage regulation and operate close to unity power factor [16], [17], [24], [26]. The same approach is adopted in this paper.

Voltage source inverters (VSI) have been widely used for DG systems. Depending on the control strategy, VSI can be classified into two types which include voltage-controlled VSI and current-controlled VSI. Voltage-controlled inverters use the output voltage and angle to control the amount of power flow while current-controlled inverters use current feedback to control the inverter's output current. A detailed comparison between the two types of VSI could be found in [27].

The control structure implemented for the grid connected DG is the synchronous reference frame control approach [26]. The DG *abc* output current is transformed into the $d-q$ axis frame to generate i_d and i_q, as shown in Fig. 1, and are compared with the reference values ($i^*_{\rm dref}$ and $i^*_{\rm qref}$) which are generated using a phase matrix transformation. The three phase voltages at the point of common coupling are inputted to a phase-locked loop to measure the frequency. The inverters should be capable of detecting an islanding situation and cease to operate during such situations [28]. This is accomplished by incorporating the SFS method with the inverter control strategy. The terms $i^*_{\rm dref}$ and $i^*_{\rm qref}$ are calculated using the current reference values ($i_{\rm dref}$ and $i_{\rm qref}$) in addition to the SFS phase angle determined by (5). This control structure is commonly associated with proportional–integral controllers due to their satisfactory behavior for regulating *dc* parameters such as the *dq* components. A detailed description of the interface control design can be found in [16] and [18].

A. Analysis of Load Versus DG Characteristic

The frequency at which an islanded system will stabilize depends to a great extent on the load and DG *phase angle–frequency* characteristic. The two main factors that determine the load characteristic are the load resonance frequency (f_r) and load quality factor (Q_f) [15]. By taking into account the load's active power frequency dependence, the load *phase angle–frequency* characteristic could be expressed as follows:

$$\phi_{\rm load}=-\tan^{-1}\left[\frac{Q_f}{(1+k_{\rm pf}(f-f_o))}\left(\frac{f_r}{f}-\frac{f}{f_r}\right)\right]. \quad (11)$$

It is noted that setting $k_{\rm pf}=0$ will yield the load phase angle characteristic presented in [15]. Fig. 2 shows the load and DG *phase angle–frequency* characteristic for a DG equipped with the SFS islanding detection method. The IEEE Std. 929 recommends testing islanding detection methods for loads with $Q_f\le 2.5$ [25]. The recent IEEE 1547.1 standard proposes testing islanding with loads having a quality factor of one [17]. In Fig. 2, the load's quality factor is varied between 0.5 and 5 while f_r and $k_{\rm pf}$ are set fixed at 60 Hz and 0.5, respectively. Based on the phase angle criterion, in order to eliminate the NDZ of the SFS method, the DG phase angle curve should be steeper (higher absolute slope) than the load phase angle curve [18]. For loads with $Q_f\ge 2$, the frequency will stabilize within the IEEE threshold values (59.3 and 60.5 Hz) and thus frequency relays will fail to detect islanding. For the case where $Q_f\ge 3$, the frequency will stabilize at 60 Hz (Point X) while for $Q_f=2$, the frequency will stabilize at approximately 59.7 Hz (Point Y). For $Q_f=0.5$ and $Q_f=1$, the SFS curve will intersect the load curve at X which is, for these loading conditions, an unstable operating point as defined by the phase

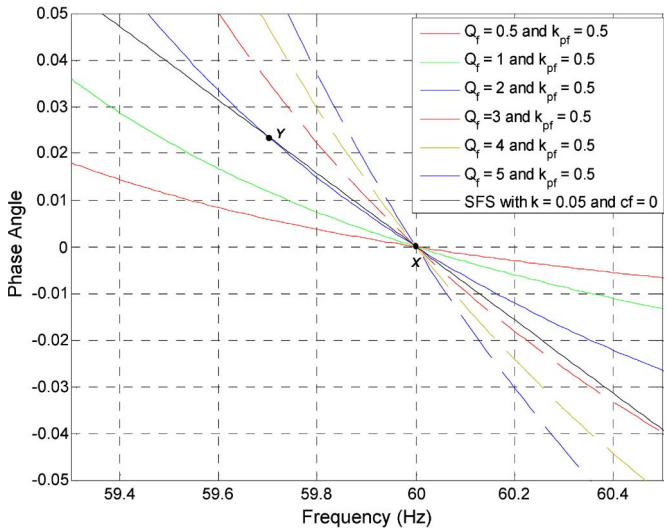

Fig. 2. Load and SFS phase angle–frequency characteristic for a load with $f_r = 60$ Hz.

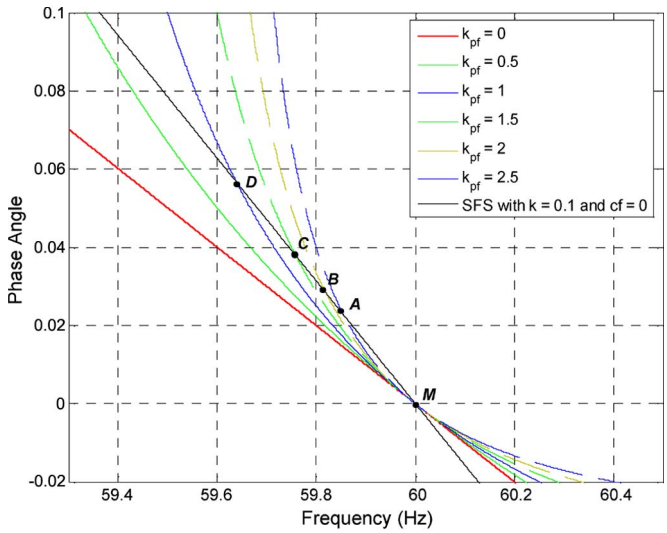

Fig. 3. Load and SFS phase angle–frequency characteristic for a load with $f_r = 60$ Hz and $Q_f = 3$ for various values of $k_{\rm pf}$.

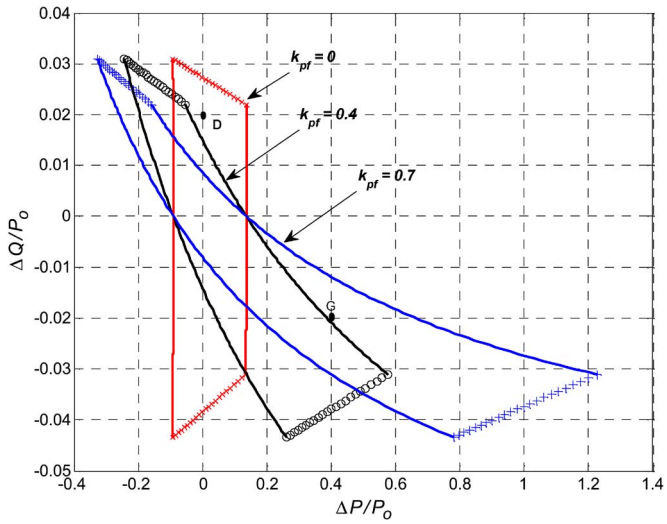

Fig. 4. NDZ for the SFS method with $cf = 0$ and $k = 0.05$ for different values of $k_{\rm pf}$ with $Q_f = 4$.

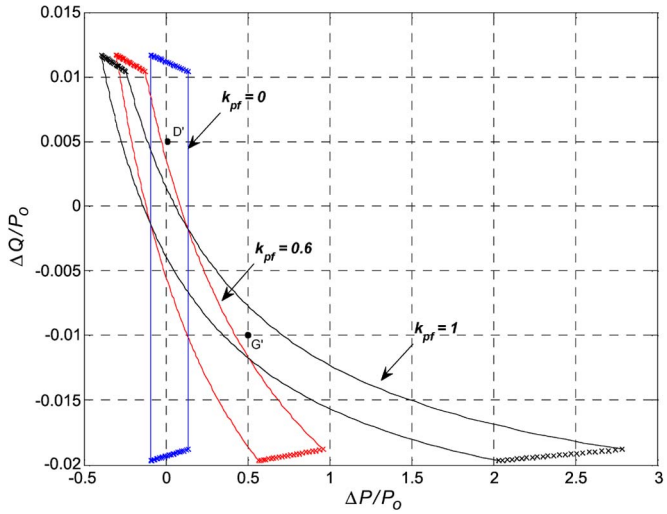

Fig. 5. NDZ for the SFS method with $cf = 0.001$ and $k = 0.005$ for different values of $k_{\rm pf}$ with $Q_f = 1$.

criterion. Similar conclusions can be drawn for cases where *cf* is nonzero.

The second parameter, that is of main focus in this paper, which has an effect on the load *phase angle–frequency* characteristic and in turn the islanding detection capability of the SFS method is $k_{\rm pf}$. Fig. 3 shows the load and DG *phase angle–frequency* characteristic for a DG equipped with the SFS islanding detection method for various values of $k_{\rm pf}$. The load Q_f is set fixed at three and f_r is set fixed at 60 Hz. For this case, *cf* is set equal to zero as in [18]. From Fig. 3, it is shown that as the value of $k_{\rm pf}$ increases the load phase angle–frequency curve becomes steeper which will in turn affect the islanding detection capability of the SFS method. For the cases under study, the SFS method will fail to operate properly and frequency relays will fail to detect islanding for values of $k_{\rm pf}$ that are greater or equal to one. The frequency will stabilize at points A, B, C, and D which are within the frequency limits. The analysis shows that the load's active power frequency dependence is an important factor to consider when designing islanding detection methods.

B. Effect of Load Frequency Dependence on NDZ

The analysis in the previous section highlighted the impact load frequency dependence can have on the islanding detection capability of the SFS method. In order to quantify this effect, the NDZ is calculated based on (8) and (10) for various values of $k_{\rm pf}$. Figs. 4 and 5 show the NDZ of the SFS under two different design cases for different values of $k_{\rm pf}$. For the two presented cases, the NDZ of the SFS method changes with the change in $k_{\rm pf}$. Without taking into account the load frequency dependence, load point "G" which corresponds to an active power mismatch of 40 kW would be considered detectable. The same loading condition would be nondetectable for $k_{\rm pf} = 0.7$. On the contrary, a load point "D," which would be nondetectable with no frequency dependence, would be detectable for $k_{\rm pf} = 0.4$ and $k_{\rm pf} = 0.7$. Similar conclusions could be

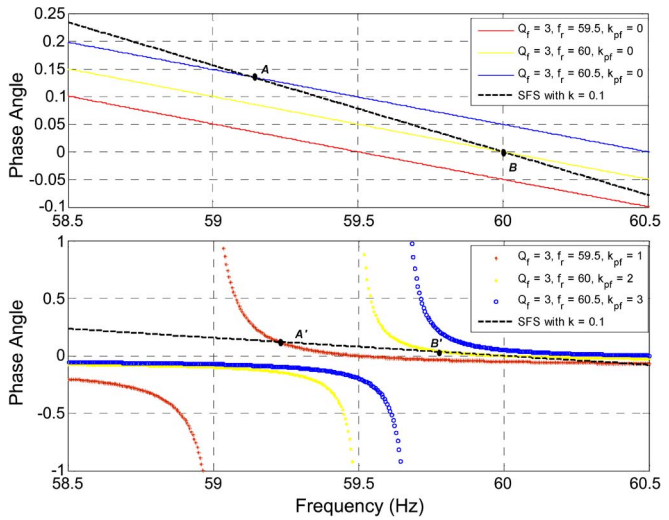

Fig. 6. Load and SFS characteristic with and without frequency dependence.

drawn for the case where $cf = 0.001$ and $k = 0.005$. The SFS method could fail to operate correctly for large active power mismatches as a result of the load's active power frequency dependence.

It is worthy to note that the presented NDZs do not take into account the transient behavior of the DG during an islanding condition. In general, islanding detection method are equipped with time delays to avoid nuisance tripping which could result from other system disturbances. Thus, the presented NDZ shown in Figs. 4 and 5 correspond to the steady-state performance. The steady-state NDZ is a conservative measure of the NDZ but the actual NDZ (taking into account transient behavior) could be smaller [8].

C. Effect of Load Frequency Dependence on the Effectiveness of the Application of Phase Angle Criterion on SFS Method

One of the main strengths of the SFS islanding detection method is the capability of eliminating the NDZ by properly setting its parameters [18]. By setting the slope of the SFS curve higher (in absolute value) than the slope of the load curve, the NDZ could be eliminated for a certain range of Q_f. This approach is known as the phase criterion approach [15], [18]. In [18], a formula for calculating the maximum expected load slope was formulated and the gain "k" of the SFS method was set higher than that value to eliminate the NDZ. Fig. 6 shows the load curves for various values of f_r with and without frequency dependence. It can be seen that for both points A and B, the SFS curve has a higher (steeper) slope than the load curve and thus both points are considered unstable operating points [18]. The slope of the load curve is almost constant within the 59.3- and 60.5-Hz window. For loads with $Q_f = 3$, the frequency is forced to drift beyond the frequency relay thresholds with k set to 0.1.

On the contrary, the slope of the load curve changes drastically within the 59.3- and 60.5-Hz frequency window with frequency dependent loads, as shown in Fig. 6. For both points A' and B', the slope of the load curve is higher (steeper) than the SFS curve. Both points are considered stable operating points and are within the frequency relay threshold values. For such loading conditions, to eliminate the NDZ using the phase criterion, the gain k of the SFS method would need to be set very high. It should be noted that the higher the gain k, the more sensitive the phase angle becomes to frequency changes which hinders the performance of the DG. This is due to the fact that large changes in phase angle will in turn induce large changes in DG reactive power output which will reduce the amount of DG active power output.

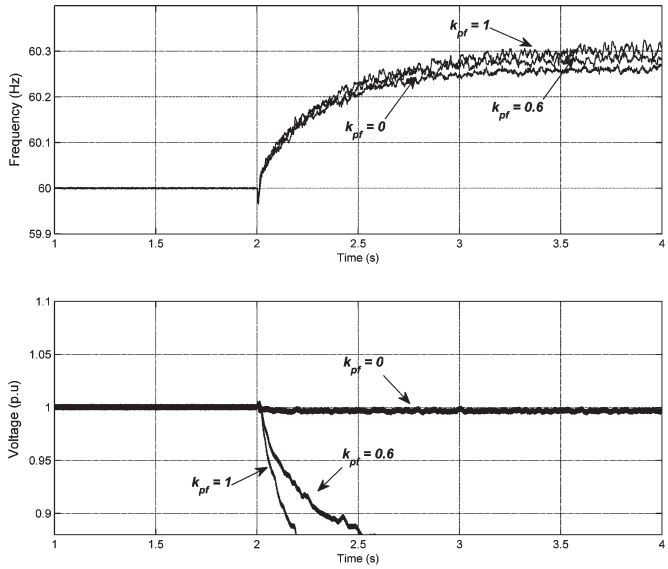

Fig. 7. Voltage and frequency deviations for the case where $\Delta P = 0$ and $\Delta Q = 0.005$ (point D' in Fig. 5).

IV. Simulation Results Highlighting the Influence of $k_{\rm pf}$ on the SFS Islanding Detection Method

The mathematical analysis and equations, provided in the previous section, prove that the load's active power frequency dependence has an impact on the performance of the SFS islanding detection method. In this section, we validate the above by implementing the system shown in Fig. 1 on PSCAD/EMTDC and testing the SFS method under various loading conditions. The resistive part is modeled as in (1) to include load frequency dependence.

A. Voltage and Frequency Deviations Under Various Active and Reactive Power Mismatch Conditions

The load frequency dependence parameter "$k_{\rm pf}$" does not only have an impact on the frequency deviation but also on the amount of voltage deviation [refer to (8) and (10)]. Figs. 7 and 8 show the frequency and voltage waveforms during an islanding condition for a DG equipped with the SFS islanding detection method. The islanding condition is initiated at $t = 2\ s$ and the load has a $Q_f = 1$. The two loading points, shown in Fig. 7, correspond to points D' and G' shown in Fig. 5. From Fig. 7, islanding could be detected easily for all cases except for the case where $k_{\rm pf} = 0$. This is in agreement with the analytical results, shown in Fig. 5, where Point D' lies within the NDZ of the SFS method for $k_{\rm pf} = 0$. Although this case study shows that loads with no frequency dependence are harder to detect,

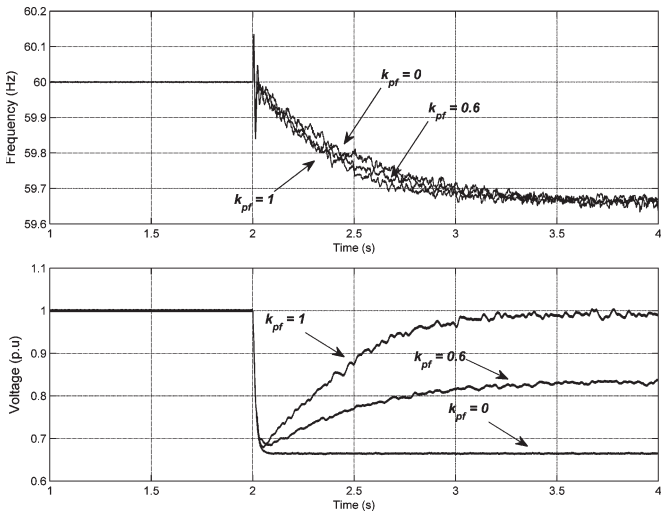

Fig. 8. Voltage and frequency deviations for the case where $\Delta P = 0.5$ and $\Delta Q = -0.01$ (point G' in Fig. 5).

this is not necessarily true for other loading conditions. By referring to Fig. 8, it is shown that all loading conditions can be detected except for the case where $k_{\rm pf} = 1$ (assuming steady state). It is worthy to note that for the case where $k_{\rm pf} = 1$, the voltage drops below the IEEE voltage threshold value due to the large active power mismatch but within approximately 500 ms the voltage stabilizes within the acceptable voltage range. As stated earlier, islanding detection methods are equipped with time delays to avoid nuisance tripping. The case where $k_{\rm pf} = 1$ would be considered detectable if the SFS method is designed with a time delay that is less than 500 ms. This issue will be highlighted in a latter section. The results obtained through the simulation model confirm and validate the mathematical analysis presented in Section III.

B. Effect of Q_f and $k_{\rm pf}$ on Islanding Detection

As highlighted earlier, the load quality factor is another parameter that will have a major effect on islanding detection. This is verified through simulation results by varying the load quality factor and initiating an islanding condition at $t = 2$ s. The load frequency dependence factor and load resonance frequency are set to 0.5 and 60 Hz, respectively. The gain "k" of the SFS method is set equal to 0.05 and the load resonance frequency is 60 Hz. Fig. 9 shows the frequency deviation during an islanding condition for a DG equipped with the SFS method. For loads with $Q_f \leq 1$, the frequency will drift beyond the threshold values. This could also be related to the analysis shown in Fig. 2 where loads with $Q_f \leq 1$ have a less steeper curve than the SFS curve. For a load with $Q_f = 2$, the frequency will stabilize at approximately 59.7 (coinciding with analytical results shown in Fig. 2) and the frequency deviation is not sufficient to trigger the frequency relay. The simulation results highlight the effect of Q_f on islanding with frequency dependent loads. For loads with $Q_f \geq 3$, the frequency will stabilize at approximately 60 Hz (corresponds to point X in Fig. 2).

To further validate the derived formulas, an islanding condition is simulated and tested for different values of $k_{\rm pf}$. The load quality factor and resonance frequency are set to 3 and 60 Hz, respectively. Similarly, an islanding condition is initiated at $t = 2$ s. Fig. 10 shows the frequency deviation for a DG equipped with the SFS method. It can be seen that, for the cases where $k_{\rm pf} = 0$ and $k_{\rm pf} = 0.5$, the frequency deviation is sufficient to operate the frequency relay. This corresponds to the results shown in Fig. 3 where the load curves do not intersect the SFS curve, at a stable operating point, within the 59.3- and 60.5-Hz window. For other loading cases, the magnitude of frequency drift is not sufficient to trigger the frequency relay. These loading conditions correspond to points A, B, C, and D in Fig. 3 which are stable operating points.

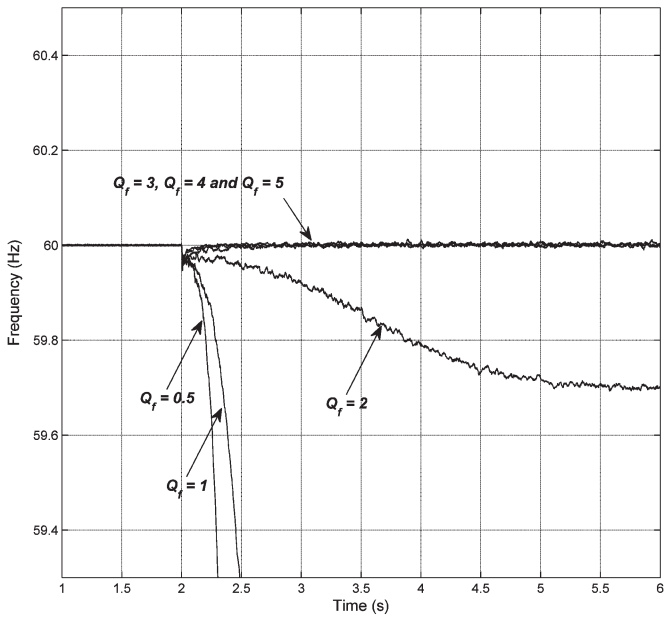

Fig. 9. Frequency deviation for a DG equipped with the SFS method under different Q_f values.

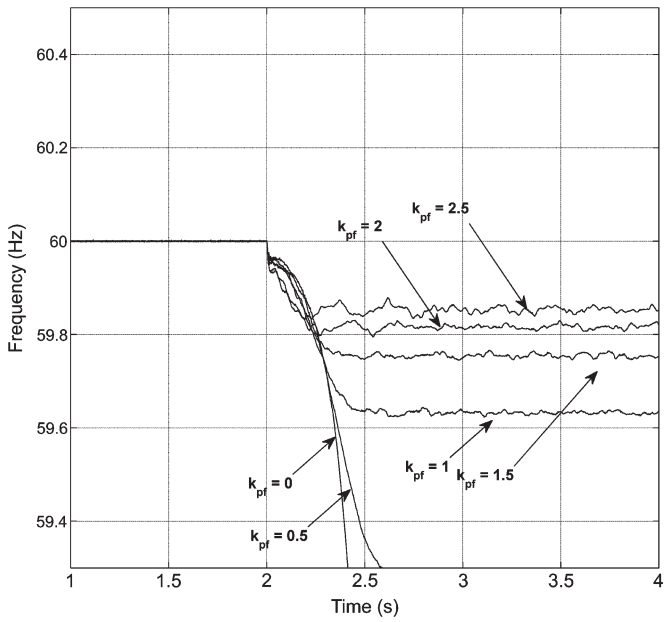

Fig. 10. Frequency deviation for a DG equipped with the SFS method $(k = 0.1)$ for different $k_{\rm pf}$ values.

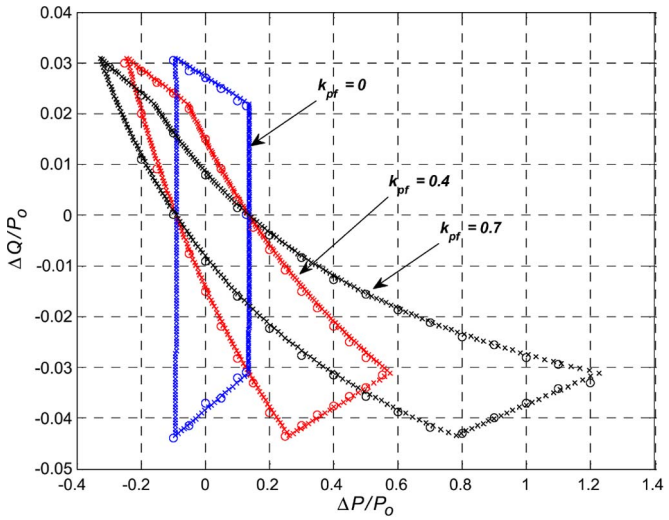

Fig. 11. Simulated (in circles) versus analytical NDZ with load frequency dependence.

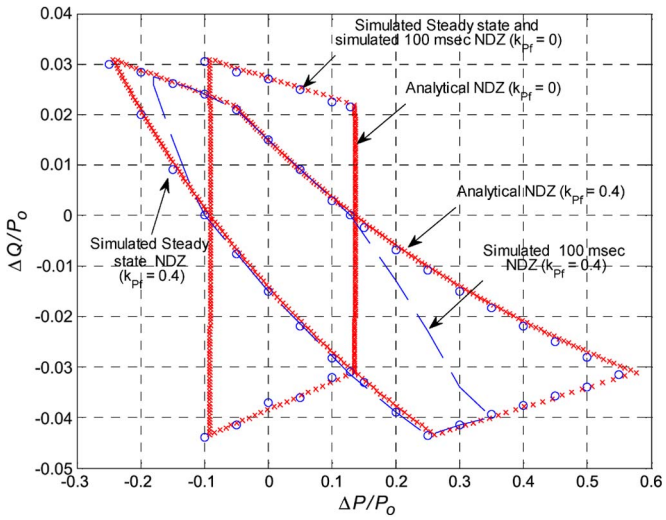

Fig. 12. Simulated 100-ms NDZ (in blue circles) versus steady-state NDZ with $cf = 0$ and $k = 0.05$.

C. Simulated Versus Analytical NDZ

In Section III, an analytical model for the NDZ of the SFS method was developed utilizing mathematical equations derived specifically to include the load frequency dependence. In this section, a simulated NDZ model is developed by repeated dynamic simulation on PSCAD/EMTDC for various values of $k_{\rm pf}$. The simulated NDZ versus the analytical NDZ is shown in Fig. 11 for a load with $Q_f = 4$. The results show a close agreement between the simulated and analytical NDZ model. Frequency dependent loads with large active power mismatches could be undetectable. In [8], it was shown and proven that the maximum active power mismatch is approximately 29.13% of the DG rated power. The results show here that the maximum active power mismatch could reach higher values depending on the load frequency dependence parameter.

The simulated NDZ shown in Fig. 11 was developed without taking into account the transient. For this reason, this NDZ will be denoted as the simulated steady-state NDZ. To take into account the transient response, repeated dynamic simulation is conducted where the voltage and frequency are monitored and the islanding detection delay time is set at 100 ms. Any voltage or frequency deviation exceeding the standard limits and lasting more than 100 ms is considered detectable. Fig. 12 shows the comparison of the simulated steady-state NDZ to the simulated 100 ms NDZ for the case where $cf = 0$, $k = 0.05$, and $Q_f = 4$. For $k_{\rm pf} = 4$, large active power mismatches ($\approx$35% of the DG capacity) are outside the simulated 100-ms NDZ. As the time delay increases, the maximum undetectable active power mismatch will increase. For the case where $k_{\rm pf} = 0$, the analytical, steady-state, and 100-ms NDZ coincide. By comparing the simulated 100-ms NDZ for $k_{\rm pf} = 0$ and $k_{\rm pf} = 0.4$, it can be seen that the load frequency dependence has an effect on the simulated 100-ms NDZ.

V. Conclusion

This paper analyzes the impact of the load's active power frequency dependence on the islanding detection capability of the SFS islanding detection method. Through mathematical and simulation analysis, it was proven that the load's active power frequency dependence has a significant impact on islanding detection and the NDZ of the SFS method. The load phase angle slope changes significantly within the IEEE threshold values and thus the application and performance of the phase criterion approach becomes limited. With load frequency dependence, the SFS method could fail to detect islanding under larger active power mismatches. The maximum undetectable active power mismatch as well as the overall NDZ will depend on the islanding detection method time delay. The simulation and analytical results prove that the load's frequency dependence is an important factor to consider when designing frequency drift islanding detection methods such as the SFS. It is envisaged that other frequency drift islanding detection methods such as the AFD and SMS methods will experience the same impacts and limitations.

References

[1] F. De Mango, M. Liserre, and A. D. Aquila, "Overview of anti-islanding algorithms for PV systems Part I: Passive methods," in *Proc. 12th Int. Power Electron. Motion Control Conf.*, Sep. 2006, pp. 1878–1883.

[2] F. De Mango, M. Liserre, and A. D. Aquila, "Overview of anti-islanding algorithms for PV systems Part II: Active methods," in *Proc. 12th Int. Power Electron. Motion Control Conf.*, Sep. 2006, pp. 1884–1889.

[3] M. Liserre, A. Pigazo, A. Dell'Aquila, and V. M. Moreno, "An anti-islanding method for single-phase inverters based on a grid voltage sensorless control," *IEEE Trans. Ind. Electron.*, vol. 53, no. 5, pp. 1418–1426, Oct. 2006.

[4] K. Tunlasakun, K. Kirtikara, S. Thepa, and V. Monyakul, "FPGA-based islanding detection for grid connected inverter," in *Proc. 30th IEEE IECON*, Nov. 2–6, 2004, vol. 2, pp. 1978–1982.

[5] H. L. Jou, W. J. Chiang, and J. C. Wu, "A simplified control method for the grid-connected inverter with the function of islanding detection," *IEEE Trans. Power Electron.*, vol. 23, no. 6, pp. 2775–2783, Nov. 2008.

[6] H. Karimi, A. Yazdani, and R. Iravani, "Negative sequence current injection for fast islanding detection of a distributed resource unit," *IEEE Trans. Power Electron.*, vol. 23, no. 1, pp. 298–307, Jan. 2008.

[7] M. Ciobotaru, V. Agelidis, and R. Teodorescu, "Accurate and less-disturbing active anti-islanding method based on PLL for grid-connected PV inverters," in *Proc. IEEE Power Electron. Spec. Conf.*, Jun. 2008, pp. 4569–4576.

[8] Z. Ye, A. Kolwalkar, Y. Zhang, P. Du, and R. Walling, "Evaluation of anti-islanding schemes based on nondetection zone concept," *IEEE Trans. Power Electron.*, vol. 19, no. 5, pp. 1171–1176, Sep. 2004.
[9] A. A. Pigazo, M. M. Liserre, R. R. A. Mastromauro, V. V. M. Moreno, and A. A. Dell-Aquila, "Wavelet-based islanding detection in grid-connected PV systems," *IEEE Trans. Ind. Electron.*, vol. 59, no. 11, pp. 4445–4455, Nov. 2009.
[10] P. Mahat, Z. Chen, and B. Bak-Jensen, "A hybrid islanding detection technique using average rate of voltage change and real power shift," *IEEE Trans. Power Del.*, vol. 24, no. 2, pp. 764–771, Apr. 2009.
[11] V. Menon and M. H. Nehrir, "A hybrid islanding detection technique using voltage unbalance and frequency set point," *IEEE Trans. Power Syst.*, vol. 22, no. 1, pp. 442–448, Feb. 2007.
[12] H. Wang, F. Lui, Y. Kang, J. Chen, and X. Wei, "Experimental investigation on non detection zones of active frequency drift method for anti-islanding," in *Proc. 33rd Annu. Conf. IEEE Ind. Electron. Soc.*, Nov. 5–8, 2007, pp. 1708–1713.
[13] F. Liu, X. Lin, Y. Kang, Y. Zhang, and S. Duan, "An active islanding detection method for grid-connected converters," in *Proc. 3rd IEEE Int. Conf. Ind. Electron. Appl.*, Jun. 3–5, 2008, pp. 734–737.
[14] M. E. Ropp, M. Begovic, A. Rohatgi, G. A. Kern, R. H. Bonn, and S. Gonzalez, "Determining the relative effectiveness of islanding detection methods using phase criteria and nondetection zones," *IEEE Trans. Energy Convers.*, vol. 15, no. 3, pp. 290–296, Sep. 2000.
[15] L. Lopes and H. Sun, "Performance assessment of active frequency drifting islanding detection methods," *IEEE Trans. Energy Convers.*, vol. 21, no. 1, pp. 171–180, Mar. 2006.
[16] X. Wang, W. Freitas, W. Xu, and V. Dinavahi, "Impact of DG interface controls on the Sandia frequency shift anti-islanding method," *IEEE Trans. Energy Convers.*, vol. 22, no. 3, pp. 792–794, Sep. 2007.
[17] *IEEE Standard for Interconnecting Distributed Resources With Electric Power Systems*, IEEE Std. 1547-2003, Jul. 2003.
[18] H. H. Zeineldin and S. Kennedy, "Sandia frequency shift parameter selection to eliminate non-detection zones," *IEEE Trans. Power Del.*, vol. 24, no. 1, pp. 486–487, Jan. 2009.
[19] H. H. Zeineldin and J. Kirtley, "Performance of the OVP/UVP and OFP/UFP method with voltage and frequency dependent loads," *IEEE Trans. Power Del.*, vol. 24, no. 2, pp. 772–778, Apr. 2009.
[20] P. Kundur, *Power System Stability and Control*. New York: McGraw-Hill, 1994.
[21] IEEE Task Force on Load Representation for Dynamic Performance, "Load representation for dynamic performance analysis," *IEEE Trans. Power Syst.*, vol. 8, no. 2, pp. 472–482, May 1993.
[22] W. J. Lee, M. S. Chen, and L. B. Williams, "Load model for stability studies," *IEEE Trans. Ind. Appl.*, vol. IA-23, no. 1, pp. 159–165, Jan./Feb. 1987.
[23] C. Hsu, "Transient stability study of the large synchronous motors starting and operating for the isolated integrated steel-making facility," *IEEE Trans. Ind. Appl.*, vol. 39, no. 5, pp. 1436–1441, Sep./Oct. 2003.
[24] *IEEE Application Guide for IEEE Std. 1547, IEEE Standard for Interconnecting Distributed Resources With Electric Power Systems*, IEEE Std. 1547.2-2008, Apr. 2009.
[25] *IEEE Recommended Practice for Utility Interface of Photovoltaic (PV) Systems*, IEEE Std. 929-2000, 2000.
[26] F. Blaabjerg, R. Teodorescu, M. Liserre, and A. Timbus, "Overview of control and grid synchronization for distributed power generation systems," *IEEE Trans. Ind. Electron.*, vol. 53, no. 5, pp. 1398–1409, Oct. 2006.
[27] S.-H. Ko, S. R. Lee, H. Dehbonei, and C. V. Nayar, "Application of voltage- and current-controlled voltage source inverters for distributed generation systems," *IEEE Trans. Energy Convers.*, vol. 21, no. 3, pp. 782–792, Sep. 2006.
[28] J. M. Carrasco, L. G. Franquelo, J. T. Bialasiewicz, E. Galván, R. C. Portillo Guisado, M. A. M. Prats, J. I. Leon, and N. Moreno-Alfonso, "Power-electronic systems for the grid integration of renewable energy sources: A survey," *IEEE Trans. Ind. Electron.*, vol. 53, no. 4, pp. 1002–1016, Jun. 2006.

H. H. Zeineldin (M'08) received the B.Sc. and M.Sc. degrees in electrical engineering from Cairo University, Cairo, Egypt, in 1999 and 2002, respectively, and the Ph.D. degree in electrical and computer engineering from the University of Waterloo, Waterloo, ON, Canada, in 2006.

He was with Smith and Andersen Electrical Engineering, Inc., where he was involved with projects involving distribution system design, protection, and distributed generation. He then worked as a Visiting Professor with the Massachusetts Institute of Technology (MIT), Cambridge. Currently, he is an Assistant Professor with the Masdar Institute of Science and Technology, Abu Dhabi, United Arab Emirates. His current interests include power system protection, distributed generation, and deregulation.

M. M. A. Salama (F'02) received the B.Sc. and M.Sc. degrees in electrical engineering from Cairo University, Cairo, Egypt, in 1971 and 1973, respectively, and the Ph.D. degree in electrical engineering from the University of Waterloo, Waterloo, ON, Canada, in 1977.

Currently, he is a Professor with the Department of Electrical and Computer Engineering, University of Waterloo. He is also currently with King Saud University, Riyadh, Saudi Arabia. His interests include the operation and control of distribution systems, cables, insulation systems, power-quality monitoring and mitigation, and electromagnetics. He has consulted widely with government agencies and the electrical industry.

Dr. Salama is a registered Professional Engineer in the Province of Ontario.